Effect of spin-dependent interactions on the two-body loss rate in ultracold ^{85}Rb collisions

Ting Xie [*]

State Key Laboratory of Molecular Reaction Dynamics, Dalian Institute of Chemical Physics,
Chinese Academy of Sciences, Dalian, Liaoning 116023, China

The spin-dependent interactions (SDIs), consisted of second-order spin-orbit coupling (SOC) and magnetic dipole-dipole interactions (MDDI), play an important role in ultracold two-body collisions for heavy atoms. We survey the inelastic two-body loss induced by SDIs in ultracold collisions of ^{85}Rb in Zeeman sublevel $|2, -2\rangle$ by using time-independent first-order perturbation theory (PT) and close-coupling (CC) approaches. The two-body loss rates from the lowest channel in $M_F = -4$ to outgoing channel $M_F = -3$ at three typical magnetic field ranges are discussed. Our calculations show PT can describe the two-body loss process well by considering the full scattering wave function even though in the region around Feshbach resonances where loss is significantly enhanced. The second-order SOC, which takes the same angular momentum coupling with MDDI, is shown to be important to ^{85}Rb two-body loss, while this term was usually omitted in previous PT calculations in some systems. Besides, our numerical results indicate the pronounced dip of two-body loss rate around 571 G mainly comes from the superposition of losses from the two lower outgoing channels in $M_F = -2$ with close minima. We also demonstrated an interesting phenomenon: the interference of two-body loss induced by the second-order SOC and MDDI. It paves an alternative way to suppress inelastic collisions through the interference between different loss causes.

I. INTRODUCTION

The formation and manipulation of molecules at ultralow temperatures has undergone tremendous progress in the past years [1]. Feshbach resonance (FR) as a most useful tool has been widely used to tune interatomic interaction in ultracold atomic collisions [2–7]. At ultralow temperature, short-range isotropic interactions have played an important role in the physics of ground state [8–10]. However, a weaker long-range anisotropic magnetic dipole-dipole interaction (MDDI) is ineligible as well and it may induce favorable Frs [11,12]. For heavy diatomic collisions, such as Rb-Cs and K-Cs, the second-order spin-orbit coupling (SOC) which has the same angular coupling with MDDI brought anisotropic collisions to be visible [13,14]. The combination of the second-order SOC and MDDI named as spin-dependent interactions (SDIs) attracts a lot of attention. Due to the dipolar coupling between incoming channel with angular momentum l to other channels with $l \pm 2$, this anisotropic interactions may have profound consequences on the properties of ultracold gases [15–18]. SDIs can also greatly modify the stability properties and may lead to new quantum phases and novel types of superfluidity [19,20].

In contrast to the beneficial aspects brought by SDIs, it is worth noting that it can induce an inelastic two-body loss to lower outgoing channels in case the incoming channel is not the energetically lowest one [21–23]. The ultracold atom samples in a magneto-optical trap may release energy during the transition from the incoming channel to a lower

outgoing channel. The released energy, which equals to the corresponding Zeeman energy levels discrepancy, is usually transferred into kinetic energy of colliding complexes that makes them "heat" and limits the sample lifetime in the trap. The two-body loss induced by SDIs has been explored by several groups. Fedichev *et al.* calculated the rates of the dipolar relaxation process for a trapped gas of metastable ^{4}He at ultracold temperature and found the sample lifetime is determined by dipolar relaxation [24]. Pasquiou *et al.* studied dipolar relaxation process in ultracold Cr atom gases and proposed several ways to control dipolar relaxation [25]. In recent years, Zhan's group measured loss rate of inelastic relaxation for higher hyperfine state combination of ^{85}Rb + ^{87}Rb in a micro-optical trap. It shows the possibility of precise test for atomic and atom-molecule collision theory [26].

^{85}Rb is a promising species for ultracold atomic gas experiments, though it has often been overlooked due to the challenges of forming a Bose-Einstein condensate (BEC) [27]. Most of works have been focused on the $|f, m_f\rangle = |2, -2\rangle$ channel due to wide resonances [28,29], where f and m_f are the total angular momentum of Rb atom and its magnetic quantum number on space z axis. Yet this channel is not the lowest one thus SDIs cause loss to three energetically lower d-wave open channels. Thompson *et al.* measured the lifetime of Fr molecules near the resonance at 155 G of Rb in $|2, -2\rangle$ and found the spontaneous dissociation driven by spin relaxation strongly depends on magnetic field [30]. Then Köhler *et al.* reproduced the observed lifetime by using the exact close-coupling (CC) method with good agreements [31], which implies CC is precise enough to characterize the loss process observed in experiment. In particular, the calculated pronounced dip in the SDIs-induced two-body loss

_____
[*]ting.xie1113@gmail.com

rate around 571 G in $|2, -2\rangle$ calculated captures our attentions as the favourable ratio between elastic and inelastic collision cross section [32]. Besides, the real part of scattering length a in this range is about $-450a_0$, where a_0 the Bohr radius. In the ultracold limit, the three-body recombination coefficient $K_3 \sim a^4$ is expected to be low and effective evaporative cooling could be achieved [33]. However, the intuitive insight on the two-body loss process, such as the cause of minimum on the loss rate, is not fully understood. Therefore an analytic method is necessary for understanding it more comprehensively. In the present work, we use an alternative first-order perturbation theory (PT) to interpret SDIs-induced loss in ultracold diatomic collisions in the presence of magnetic field. The first-order PT, also known as Fermi's golden rule, is already shown to be an efficient and intuitive tool in a simple two-channel problem with weak coupling [34–36]. Here we extend it to multiopen channel scattering problem and apply it in the ultracold ^{85}Rb collisions.

This paper is organized as follows. In Sec. II, we briefly introduce two kinds of numerical methods for determine the SDIs-induced two-body loss parameter, including the CC and PT approaches. In Sec. III, we discuss the two-body loss in ^{85}Rb $|2, -2\rangle$ ultracold collisions at three typical magnetic fields to verify PT validity. The two-body loss rate dip around 571 G is analyzed as well. Finally, a conclusion is drawn in Sec. IV.

II. THEORY

The Hamiltonian for the interaction of two alkali-metal atoms in the presence of a static magnetic field can be written as

$$\frac{\hbar^2}{2\mu}\left[-R^{-1}\frac{d^2}{dR^2}R + \frac{l(l+1)}{R^2}\right] + \hat{h}_1 + \hat{h}_2 + \hat{V}(R), \quad (1)$$

where μ is the reduced mass, R is the nuclear separation, and l is the orbital quantum number between two atoms. The interenergy Hamiltonian, $\hat{h}_1$ and $\hat{h}_2$, are given by

$$\hat{h}_j = \zeta \hat{i}_j \cdot \hat{s}_j + g_s \mu_B B m_{s_j} + g_n \mu_B B m_{i_j}, \quad (2)$$

where ζ is the atomic hyperfine constant; $\hat{s}_j$ and m_{s_j} are the electron spin and electron spin projection on the quantisation axis, respectively; $\hat{i}_j$ and m_{i_j} are the nuclear spin and its projection, respectively; g_s and g_n are the electronic and nuclear g factors, respectively; μ_B is the Bohr magneton; and B is the external magnetic field. The interaction between the two atoms is given by the potential term $\hat{V}(R)$

$$\hat{V}(R) = \hat{V}_c(R) + \hat{V}_{sd}(R), \quad (3)$$

where $\hat{V}_c(R) = V_0(R)\hat{\mathcal{P}}^{(0)} + V_1(R)\hat{\mathcal{P}}^{(1)}$ is an isotropic potential operator that depends on the singlet and triplet potential energy curves $V_0(R)$ and $V_1(R)$. $\hat{\mathcal{P}}^{(0)}$ and $\hat{\mathcal{P}}^{(1)}$ project onto singlet and triplet subspaces, respectively.

The spin-dependent interactions $\hat{V}_{sd}(R)$ can be expressed as

$$\hat{V}_{sd}(R) = \lambda(R)[\hat{s}_1 \cdot \hat{s}_2 - 3(\hat{s}_1 \cdot \vec{e}_R)(\hat{s}_2 \cdot \vec{e}_R)]$$
$$= \hat{V}_{so}(R) + \hat{V}_{dd}(R), \quad (4)$$

where $\vec{e}_R$ is a unit vector along the interatomic axis and $\lambda(R)$ is an R-dependent coupling constant,

$$\lambda(R) = E_h \alpha^2 \left[A_{so} \exp(-\beta_{so}((R - R_0)/a_0)) + \frac{1}{(R/a_0)^3}\right], \quad (5)$$

where $\alpha \approx 1/137$ is the atomic fine-structure constant and a_0 the Bohr radius. β_{so} and R_0 of Rb are adopted from theoretical calculations by Mies *et al.* [15] and A_{so} was determined in Ref. [37]. The two terms inside brakes represent the radial formulas of the second-order SOC and MDDI, respectively. Since the radial part of $\hat{V}_{so}$ is exponential decayed with R and it vanishes quickly when the diatomic distance is beyond the van der Waals interaction well, it is refereed to the short-range interaction in our work. Similarly, $\hat{V}_{dd}$ represents the long-range part of $\hat{V}_{sd}$ and it can be treated as 0 when $R > 5000\, a_0$.

A. K_2 from CC calculations

Inelastic collisions occur when outgoing channels are present. The elastic scattering S-matrix element of incoming channel e can be written in terms of a complex phase shift δ_e as

$$S_{ee} = e^{i\delta_e}. \quad (6)$$

For any collision energy E, the two-body loss rate coefficient is

$$K_2 = \frac{\pi\hbar}{\mu k}\sum_i |S_{ei}(E)|^2, \quad (7)$$

where k is the wave vector, E is the collision energy, and S_{ei} is represents the nondiagonal S-matrix element. The index i ranges over all open channels other than the incoming channel e. In the low-energy limit, the complex phase shift translates into a complex scattering length

$$a = \alpha - i\beta, \quad (8)$$

where α and β represent the real and imaginary parts of the scattering length, respectively. Note that in this formula i represents imaginary unit. We introduce a parameter a_{res}, which characterizes the strength of the resonance. Across a Fr α in scattering length displays an oscillation of magnitude $a_{res}/2$ and β shows a corresponding peak of height a_{res}. An alternative way of finding K_2 is to extract it from β, using the following formula:

$$K_2 = \frac{2h}{\mu}g_n\beta, \quad (9)$$

where $g_n = 2$ for a thermal gas of identical bosons, and 1 others.

In the present work, we obtained scattering matrix S and scattering length principally from CC calculations. We introduce the symmetrized basis set

$$|s_1 m_{s1} i_1 m_{i1} s_2 m_{s2} i_2 m_{i2}|lm_l\rangle$$
$$= \frac{1}{\sqrt{2(1 + \delta_{m_{s1}m_{s2}}\delta_{m_{i1}m_{i2}})}}\{|s_1 m_{s1} i_1 m_{i1} s_2 m_{s2} i_2 m_{i2}\rangle$$
$$+ \eta|s_2 m_{s2} i_2 m_{i2} s_1 m_{s1} i_1 m_{i1}\rangle\}|lm_l\rangle, \quad (10)$$

where m_l is the orbital angular momentum projection onto the quantization axis and $\eta = \pm 1$ which describe the symmetrized and antisymmetrized wave functions, respectively. In our work, only $\eta = 1$ is used as we are considering indistinguishable particles with identical initial states. By introducing SDIs the total angular momentum projection $M_{\mathcal{F}}$ is a good quantum number, where $M_{\mathcal{F}} = M_F + m_l$ and M_F is the projection of total electronic and nuclear spins. We solved the coupled Schrödinger equations with full Hamiltonian in Eq. (1) by using the MOLSCAT package [38], then the S matrix and two-body loss rate were extracted when the log-derivative matrix propagation ended in long range.

B. K_2 from first-order PT

The first-order PT has been applied to explore the dipolar relaxation in ultracold Cr and spin-polarized $^4\text{He}^*$ diatomic collisions [21,24]. By ignoring all effects of the short-range molecular potentials, Hensler *et al.* modeled the dipolar loss well at relative low magnetic fields [21]. However, Pasquiou *et al.* proved that at relatively high magnetic fields the molecular potentials have a significant influences [25]. Here we introduce the first-order PT by considering the exact molecular potentials.

The two-body loss rate in PT can be represented as

$$K_2 = 2\pi \sum_i \left| \langle \Psi_{\text{in}} | \hat{V}_{\text{sd}} | \Psi_{\text{out}}^i \rangle \right|^2, \tag{11}$$

where Ψ_{in} and Ψ_{out}^i denote the incoming and ith outgoing channel wave functions, respectively. It is important to note that in the presence of magnetic field, $\Psi_{\text{in(out)}}$ no longer expresses the individual open channel wave function of incoming (outgoing) channels. As the internal energy Hamiltonian couples the open and closed channels, the wave functions in closed channels may becomes significant when close to Frs. Therefore we should adopt full-scattering wave functions, which are the linear combination of channel wave functions in terms of single M_F in calculations. In the spin basis, one can write the full scattering wave functions as

$$\Psi_{\text{in(out)}}^{M_F} = \sum_{j=1,N} C_j \psi_{\text{in(out)}}^j |s_1 m_{s1} i_1 m_{i1} s_2 m_{s2} i_2 m_{i2}\rangle |l m_l\rangle, \tag{12}$$

where N is the channel number in incoming or outgoing M_F, $\psi_{\text{in(out)}}^j$ stands for the energy-normalized radial wave function associated with channel jth, and C^j denotes the corresponding normalized coefficient in angular basis which is already symmetrized. Usually we use field dressed hyperfine state $|f_1, m_{f1}; f_2, m_{f2}\rangle$ to label the incoming and outgoing channels, then Eq. (12) can be rewritten as

$$\Psi_{\text{in(out)}}^{M_F} = \sum_{j'=1,N} C'_{j'} \psi_{\text{in(out)}}^{j'} |f_1 m_{f1}; f_2 m_{f2}\rangle |l m_l\rangle, \tag{13}$$

where $C'_{j'}$ and $\psi_{\text{in(out)}}^{j'}$ are the angular normalized coefficients and the wave functions in field dressed hyperfine state basis. We can go from one basis to another basis using angular momentum algebra. As full-channel wave functions are considered here, the two-body loss rate does not rely on the basis we choose. However, K_2 will greatly depend on the basis set if any approximation on the channels is taken into account.
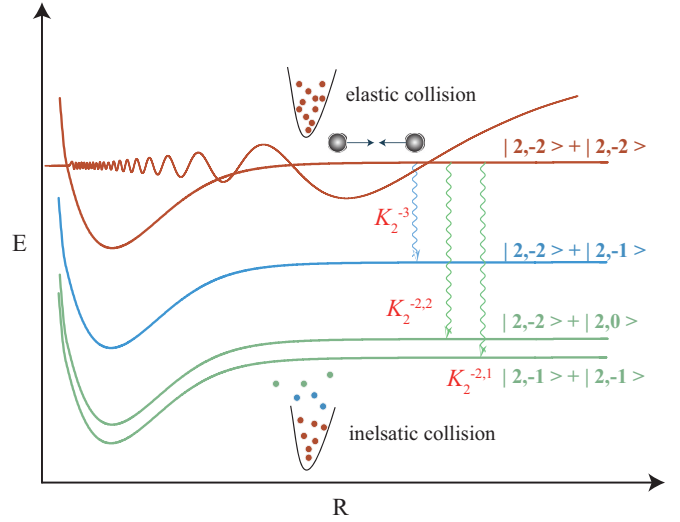

FIG. 1. Colliding ^{85}Rb atoms interact between incoming (brown) and outgoing (light-blue and green) channels by considering SDIs with l up to 2. The ^{85}Rb atoms are prepared in the incoming channel $|2, -2\rangle + |2, -2\rangle$, which can be coupled to three lower outgoing channels. The atoms transited to the lower outgoing channels through SIDs, which can lead to "hot" atoms and may cause atom loss. The two-body loss rates to outgoing channels in $M_F = -2$ are labeled as $K_2^{-2,1}$ and $K_2^{-2,2}$ where the superscript -2 means M_F and the following number 1(2) is used to distinguish two different channels. As there is only one outgoing channel in $M_F = -3$ therefor we take the notation K_2^{-3}.

There are several numerical approaches to obtain scattering wave functions from exact molecular potentials, such as logarithmic derivatives [39], renormalized Numerov [40], and Mapper-Fourier-Grid Hamiltonian (MFGH) [41] methods. In this work, we solve $\psi_{\text{in(out)}}$ by using the MFGH method which has been proved to be an efficient and precise method to study diatomic collisions at ultralow temperature and was widely used for investigating photoassociation process [42–48]. We obtain the incoming (outgoing) wave functions in correlated M_F by solving the time-independent Schördinger equations with the Hamiltonian in Eq. (1) but no SDIs. Then we can calculate the two-body loss rate by taking $\hat{V}_{\text{sd}}(R)$ as the perturbative interaction in terms of Eq. (11).

III. RESULTS AND DISCUSSIONS

In this work, we investigate two-body loss of ^{85}Rb in $|2, -2\rangle$ channel in s-wave collisions at ultralow limit where the scattering length and two-body loss rate do not depend the collision energy. Higher partial waves in incident channel are neglected since their contributions are negligible compared to s-wave [25]. The ground singlet and triplet Hund case a potentials of $^{87}\text{Rb}_2$ come from the analytical expression produced by Struss *et al.* based on spectroscopy data [37]. We apply them in $^{85}\text{Rb}_2$ by using mass scaling without any correction.

Figure 1 depicts the inelastic scattering process in ultracold Rb atoms colliding in $|2, -2\rangle$ channel under the action of magnetic field. Since $M_{\mathcal{F}} = -4$ is conserved by considering SDIs, the incoming channel is coupled to three d-wave
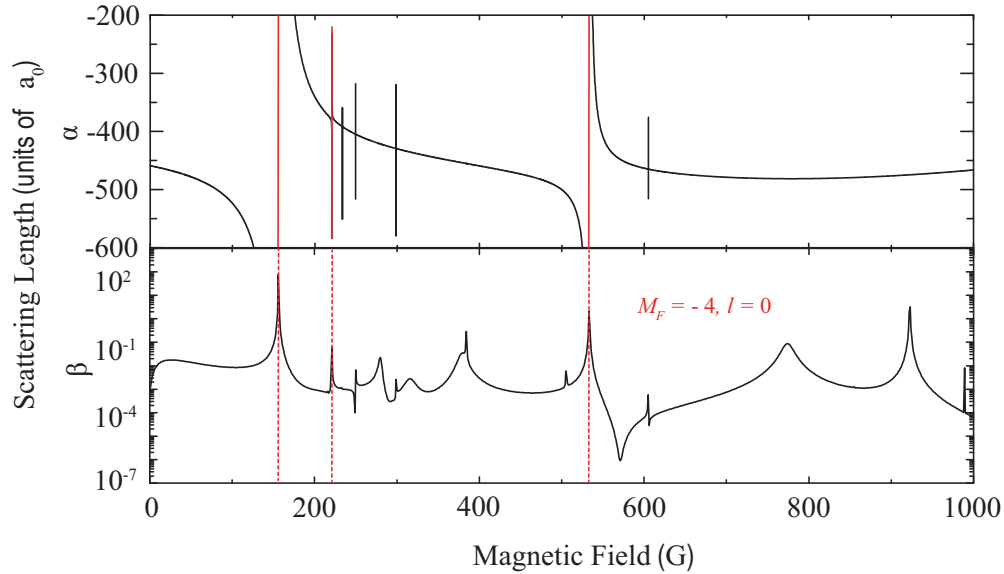
FIG. 2. The calculated s-wave scattering length in $|2, -2\rangle + |2, -2\rangle$ of ultracold ^{85}Rb collisions with CC method, by including SDI with l up to 2. In the field range $0 \sim 1000$ G, only three Frs are induced by s-wave bound states of $M_F = -4$ whose resonant positions are labeled with red lines, while the others appeared only when SDIs are included. It should be noted that some resonances are not evident in α but strongly decayed in β.

outgoing channels which are $|2, -2\rangle + |2, -1\rangle$, $|2, -2\rangle + |2, 0\rangle$, and $|2, -1\rangle + |2, -1\rangle$, respectively. The collision happened with $M_F = -4$ unchanged is usually called elastic collision. While inelastic collisions occur because of the release of internal energy into the motion when colliding atoms end up in a lower internal state. The gain in kinetic energy is on the order of the Zeeman and hyperfine energy, depending on the inelastic channel, and generally causes "hot" atoms thus limit the colliding complex lifetime in magnetic-optical trap. Hence the resonances become decayed and the imaginary part of scattering length is enhanced. Figure 2 shows the calculated real and imaginary parts of $a(B)$ for s-wave collisions in $|2, -2\rangle$ channel by using CC method. We found 11 resonances with $a_{\text{res}} > 1.0\, a_0$ from $0 \sim 1000$ G. Two of them, the resonances at 155 and 532 G, are induced by s-wave bound states of $M_F = -4$ and exhibit big polelike feature in α. By contrast, the resonances due to d-wave bound states show much narrower profiles. The imaginary part β related to two-body loss rate reveals rapidly increased feature around resonance as well. Additionally, the remarkable fact that more evident resonant features in β than α indicates narrow resonance could be detected through measuring two-body loss rates in experiment.

By comparing the theoretical resonance positions with those observed in ^{85}Rb experiment [32], we show CC method is precise enough to predict resonance features based on exact molecular potentials. An alternative way for studying multichannel colliding system is MFGH method. It was widely used to study the photoassociation process [49,50], then is developed by Pellegrini *et al.* to explore Feshbach-optimized photoassociation [42]. The advantage of MFGH is we are able to observe the wave functions in every channel directly and extract the associated scattering parameters. For example, in low-energy limit, the real part of scattering length α equals $\tan(kR_n)/k$, where k is the wave vector and R_n the position

of the wave function equaling to 0 at a large distance in the incoming channel. Table I lists the parameters of resonances induced by $M_F = -4$ s-wave bound states. One can find the accuracy for MFGH method is surprising and expected to offer us the precise wave functions.

A. Single outgoing channel case

As mentioned in Sec. II, the PT has been used to estimated the Cr dipolar loss and shows a good agreement with experimental results at low magnetic fields [25]. However, in vicinity of Fr, the inelastic loss is dramatically enhanced, thus it is interesting to test the reliability of PT method at different fields. At the beginning, we will check the validity of improved PT in three typical regions: low magnetic fields, near Fr, and high magnetic fields. Noting that near the Frs induced by SDIs PT never works. Since SDIs is treated perturbatively and wave functions in incoming and outgoing channels are calculated separately in PT theory, we cannot observe the amplification of short-range wave functions in incoming or

TABLE I. Positions and widths of Frs for ^{85}Rb in $|2, -2\rangle + |2, -2\rangle$ in the field range $0 \sim 1000$ G. All resonances shown are induced by s-wave bound states. The experimental values are taken from Ref. [32]. The Fr positions and widths calculated by MFGH are fitted from the scattering length extracted from the scattering wave function in incoming channel.

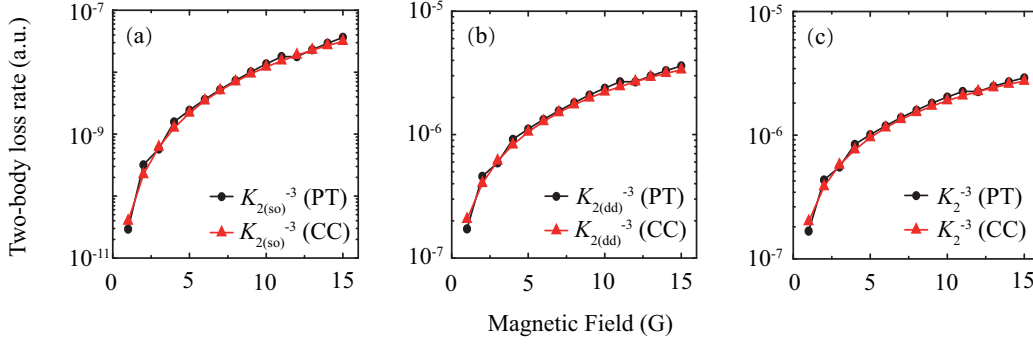| Incoming s-wave $|2, -2\rangle + |2, -2\rangle$ state					
Experiment		CC		MFGH	
B_0 (G)	δ (G)	B_0 (G)	Δ (G)	B_0 (G)	Δ (G)
156	10.5(5)	155.3	10.90	154.7	10.54
219.58	0.22(9)	219.9	0.0091	219.4	0.0086
532.3	3.2(1)	532.9	2.30	532.2	2.43

FIG. 3. The calculated two-body loss rate related to outgoing channel $M_F = -3$ at low magnetic fields. The black and blue lines represent the results by using PT and CC method, respectively.

outgoing channels in this range hence no enhancement feature in $K_2(\text{PT})$. In the next discussions, we will avoid the regions in connection with SDIs-induced Frs.

For the case illustrated in Fig. 1, there are three outgoing channels, two of which belong to $M_F = -2$ and another one in $M_F = -3$. For simplifying the discussion, we only consider the loss to outgoing channel $M_F = -3$ for examinations. We expect this simple model of two open channels could give us a straightforward insight on the loss and we will extended it to more complicated multioutgoing channels in the following part.

As $\hat{V}_{sd}$ can be decomposed into $\hat{V}_{so}$ and $\hat{V}_{dd}$, we can look into their characters in K_2 separately. Since the plotted radial wave functions are real in our calculations, one can rewrite two-body loss rate related to outgoing channel $M_F = -3$ as following:

$$
\begin{aligned}
K_2^{-3} &= 2\pi \left| \langle \Psi_{\text{in}}^{-4} | \hat{V}_{\text{so}} + \hat{V}_{\text{dd}} | \Psi_{\text{out}}^{-3} \rangle \right|^2 \\
&= 2\pi \left| \langle \Psi_{\text{in}}^{-4} | \hat{V}_{\text{so}} | \Psi_{\text{out}}^{-3} \rangle \right|^2 + 2\pi \left| \langle \Psi_{\text{in}}^{-4} | \hat{V}_{\text{dd}} | \Psi_{\text{out}}^{-3} \rangle \right|^2 \\
&\quad + 4\pi \langle \Psi_{\text{in}}^{-4} | \hat{V}_{\text{so}} | \Psi_{\text{out}}^{-3} \rangle \langle \Psi_{\text{in}}^{-4} | \hat{V}_{\text{dd}} | \Psi_{\text{out}}^{-3} \rangle \\
&= K_{2(\text{so})}^{-3} + K_{2(\text{dd})}^{-3} \pm 2\sqrt{K_{2(\text{dd})}^{-3} * K_{2(\text{so})}^{-3}},
\end{aligned}
\tag{14}
$$

where Ψ_{in}^{-4} and Ψ_{out}^{-3} represent the full scattering wave functions in $M_F = -4$ and -3, respectively. $K_{2(\text{so})}^{-3}$ and $K_{2(\text{dd})}^{-3}$ describer the loss caused by $\hat{V}_{\text{so}}$ and $\hat{V}_{\text{dd}}$, separately. The term in square root denotes the interference between them and its sign is the same as the product of $\langle \Psi_{\text{in}} | \hat{V}_{\text{so}} | \Psi_{\text{out}} \rangle$ and $\langle \Psi_{\text{in}} | \hat{V}_{\text{dd}} | \Psi_{\text{out}} \rangle$.

We plot the calculated two-body loss rate K_2^{-3} from 1 to 15 G in Fig. 3. One can find the PT results agree with CC calculations very well. In this range, $K_{2(\text{so})}^{-3}$ is very small compared to $K_{2(\text{dd})}^{-3}$, which is because the amplitudes of the radial wave functions in short range for both ψ_{out} and ψ_{in} are very small. More often than not, neglecting the contribution of $\hat{V}_{\text{so}}$ to K_2 will not cause serious problem at low magnetic fields. The tiny difference between two methods mainly comes from the precision of wave function obtained by MFGH. For CC method, the loss rate is calculated with a constant collision energy. However, for MFGH, the collision energies corresponding to calculated scattering states are associated with the size of box [41]. In our calculation, we set the max interatomic distance as 10000 a_0 by considering the computation and

precision. If it is large enough, the energy density of scattering states would be very high and we can obtain the wave functions with an energy much close to that certain one. Then PT results are believed to be in full accordance with that of CC.

Near a Fr the inelastic loss is strongly enhanced since the scattering wave functions in short range are amplified. While the SDIs remain weak and PT is expected to be stood. Here we checked its validity near the wide resonance at 155 G. Figure 4 displays the calculated two-body loss rates to $M_F = -3$ from 158 to 180 G. One can find the discrepancy between two methods becomes large when close to Fr. It mainly arises from the fact: for the Fr at 155 G, the resonance position calculated by MFGH has a deviation of -0.6 G compared to CC method which can be seen from Table I. The corresponding dip in two-body loss rate K_2^{-3} follows this deviation and large discrepancy occurs. If the resonance position by MFGH is closer to CC, we hold that the discrepancy of loss minimum position in two methods will reduce more. Moreover, one can find the minimum of K_2^{-3} is different from that of $K_{2(\text{so})}^{-3}$ and $K_{2(\text{dd})}^{-3}$, which can be readily comprehended with PT method. In terms of Eq. (14), if $K_{2(\text{so})}^{-3}$ is close to $K_{2(\text{dd})}^{-3}$ and $\langle \Psi_{\text{in}} | \hat{V}_{\text{so}} | \Psi_{\text{out}}^{-3} \rangle \times \langle \Psi_{\text{in}} | \hat{V}_{\text{dd}} | \Psi_{\text{out}}^{-3} \rangle$ is negative, K_2^{-3} is approaching 0. We are able to reach a conclusion that the minimum of K_2^{-3} is determined by both $\hat{V}_{\text{so}}$ and $\hat{V}_{\text{dd}}$. It also implies the interference between $K_{2(\text{so})}$ and $K_{2(\text{dd})}$ is much interesting and we could estimate the second-order SOC strength by utilizing the observed two-body loss rate minimum in experiment.

At last we plot the two-body loss rate related to outgoing channel $M_F = -3$ at field from 795 to 805 G in Fig. 5. We look into this field range since the Zeeman sublevel energy splitting between incoming and outgoing channels is over 400 MHz which may cause a temperature variation of ultracold atoms sample up to 20 mK. It is much larger than the magnetic-optical trap depth, therefor the two-body loss rate at high fields is more essential than lower field. In the field range illustrated in Fig. 5, no Fr and α is approximately the background scattering length. Our calculations on K_2^{-3} shows a good consistence between two methods. The difference of magnitude order in Figs. 5(a) and 5(b) indicates the important role of second-order SOC in two-body loss in ultracold ^{85}Rb scattering. The degrees of deviations on $K_{2(\text{so})}^{-3}$ and $K_{2(\text{dd})}^{-3}$ are different between two methods, yet they are eliminated in K_2^{-3} due to the interference term at these fields.
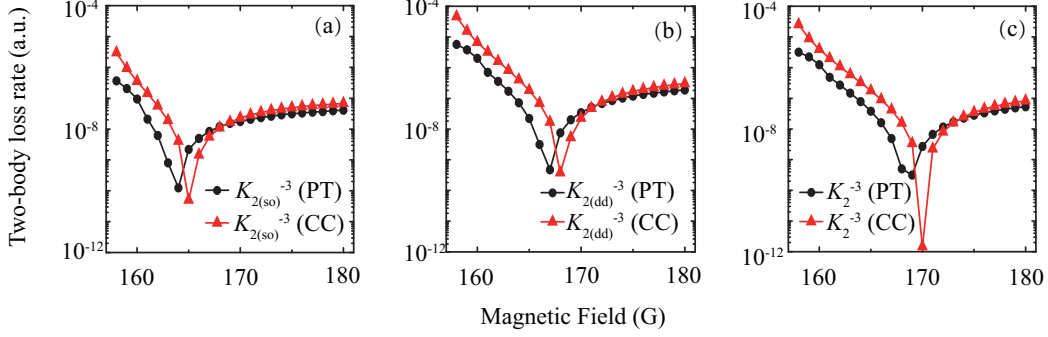
FIG. 4. The calculated two-body loss rates related to outgoing channel $M_F = -3$ near the wide Fr at 155 G. The black and red lines represent the results by using PT and CC methods, respectively. Note that the minims appeared in these lines do not exist if $M_F = -2$ included.

Through the above calculations we demonstrated PT could give us reliable results on SDIs-induced two-body loss even though for the fields near Frs in our two open channels model. We also showed the interference between $\hat{V}_{so}$ and $\hat{V}_{dd}$ could cause a minimum in inelastic collisions while the elastic collisions are unaffected. At present, since the techniques of suppression inelastic collisions are devoted to preventing atomic or molecular interactions in short range [51,52], our calculations suggests we may suppress it through introducing another adjustable loss process in which coupling rules are similar with that of original loss path in a simple two open-channel model.

B. Multioutgoing channels case

In the following, we extend the above two open channels calculations to real case by considering outgoing channels in $M_F = -2$. We survey the two-body loss rate at the fields from 565 to 580 G where β exhibits a big deep around the broad resonance at 532 G. This field range is interesting since it supplies us a magnetic region for cooling due to more favorable elastic to inelastic ratio based on CC calculations.

By considering all the channels in $M_{\mathcal{F}} = -4$, the total two-body loss rate turns into the sum of loss from all outgoing channels,

$$K_2 = 2\pi \left| \langle \Psi_{in}^{-4} | \hat{V}_{sd} | \Psi_{out}^{-3} \rangle \right|^2 + 2\pi \left| \langle \Psi_{in}^{-4} | \hat{V}_{sd} | \Psi_{out}^{-2} \rangle \right|^2$$
$$= K_2^{-3} + K_2^{-2}, \tag{15}$$

where Ψ_{out}^{-2} and K_2^{-2} represent the scattering wave functions and two-body loss rate to $M_F = -2$, respectively. Note we assume no interference between the $M_F = -3$ and -2 open channels as the coupling between them is very weak and we are able to sum the loss to different channels together. Due to two open channels in $M_F = -2$ we can further rewrite K_2^{-2} as the sum of $K_2^{-2,1}$ and $K_2^{-2,2}$, which describe the losses to the open channels in $M_F = -2$ as illustrated in Fig. 1. In this case, we need two sets of d-wave wave functions to describe different open channel scattering with the same total energy in $M_F = -2$. MFGH cannot give us two wave functions with exactly the same scattering energy, yet by using big box size we can always find twinning scattering states with similar energy. In the calculation we treat the twinning states as the sets of $\psi^{-2,1}$ and $\psi^{-2,2}$ which specify the radial wave functions of open channel in $|2, -2\rangle + |2, 0\rangle$ and $|2, -1\rangle + |2, -1\rangle$, respectively. For an instance, in Fig. 6, we plot the energy-normalized wave functions of open channels of $M_F = -2$ in short range at 571 G to show the difference between $\psi^{-2,1}$ and $\psi^{-2,2}$. The wave functions in long range consist very well with energy-normalized bessel functions and not shown here. For both open channels of $M_F = -2$ in d-wave no shape resonance or Fr near 571 G, we only exhibit the wave functions in open channels due to relatively large amplitudes. One can find the profiles of wave function in two panels are very similar despite of the phase. $\psi^{-2,1}$ ($\psi^{-2,2}$) exhibits big amplitude only when $|2, -2\rangle + |2, 0\rangle$ ($|2, -1\rangle + |2, -1\rangle$) is the exit channel. Besides, we observed
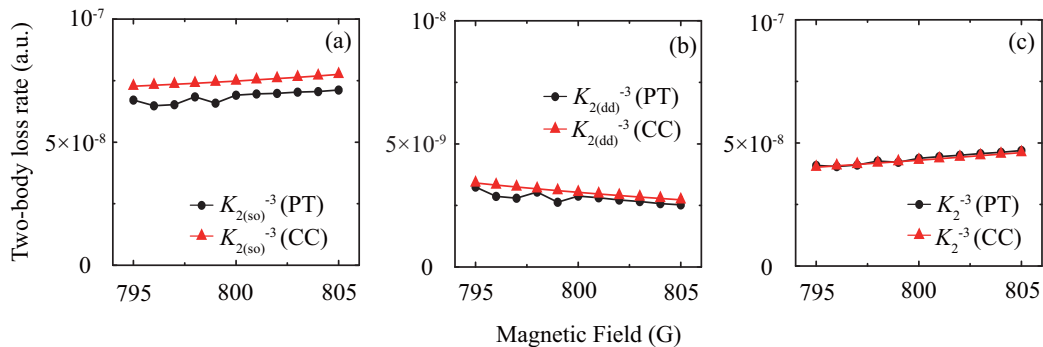

FIG. 5. The calculated two-body loss rates relate to outgoing channel $M_F = -3$ in the range from 795 to 805 G. The black and red lines represent the results by using PT and CC methods, respectively.
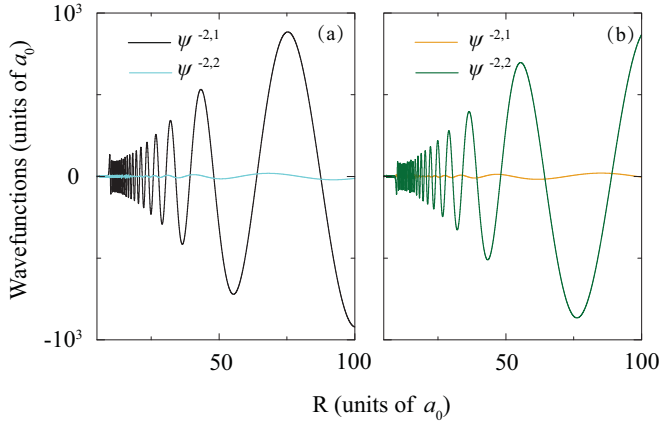
FIG. 6. The energy-normalized wave functions in two outgoing channels of $M_F = -2$ at 571 G, where $\psi^{-2,1}$ and $\psi^{-2,2}$ specify the wave functions of lower and higher open channels in $M_F = -2$, respectively. (a) Illustrates the corresponding wave functions when the lower open channel in $M_F = -2$ as the outgoing channel. Similarly, (b) shows the wave functions when the higher open channel in $M_F = -2$ as the outgoing channel.

the amplitude of wave functions of $\psi^{-2,1}$ on left panel and $\psi^{-2,2}$ on right one are nearly the same. It indicates the loss to both two open channels are expected to have close values at this field. It is worth noting that the subequal $K_2^{-2,1}$ and $K_2^{-2,2}$ do not produce minimum in K_2^{-2} since we do not consider the interference between the two open channels in $M_F = -2$.

After obtaining the wave functions we calculated the two-body loss rates to different open channels in $M_F = -2$ from 565 to 580 G displayed in Fig. 7(a). The close minimum positions in $K_2^{-2,1}$ and $K_2^{-2,2}$ shows the properties of two open channels are very similar since the collision energy in incoming channel is very high relatively to both open channels in $M_F = -2$. One can also find the minimum of K_2^{-2} by PT method is 10^{-9} a.u. at 571 G while it is 10^{-11} a.u. in CC calculation. This magnitude order difference probably comes from two aspects. Firstly the hypothesis that no interference between the open channels in $M_F = -2$ may be not exactly true as the two open channels are coupled together via Zeeman and hyperfine interactions. Hence we need to introduce a term describing the interference between $K_2^{-2,1}$ and $K_2^{-2,2}$ in K_2^{-2} calculations. Secondly as we illustrated in Fig. 6, the wave functions of two open channels are very similar. However, we cannot produce $\psi^{-2,1}$ and $\psi^{-2,2}$ with exactly the same total energy due to the limitation of MFGH and thus the loss rate are not precisely enough. It is an interesting point we would explore in future. Figure 7(b) presents the calculated two-body loss rates to open channels in $M_F = -2$ and -3 and total loss rate K_2. In this range, K_2^{-2} is much larger than K_2^{-3} which contributes little to total loss rate in terms of PT calculations. By comparing the two curves of K_2(CC) and K_2(PT), we can find their difference is much smaller than the curves of K_2^{-2} shown in Fig. 7(a). It is because K_2^{-3}(CC) is larger than K_2^{-3}(PT) and K_2^{-2}(CC) is smaller than K_2^{-2}(PT), so the difference in K_2 becomes smaller. Besides, we calculated the loss to $M_F = -2$ and -3 open channels from 0 to 1000 G with CC approach and found K_2^{-3} is always smaller than K_2^{-2}
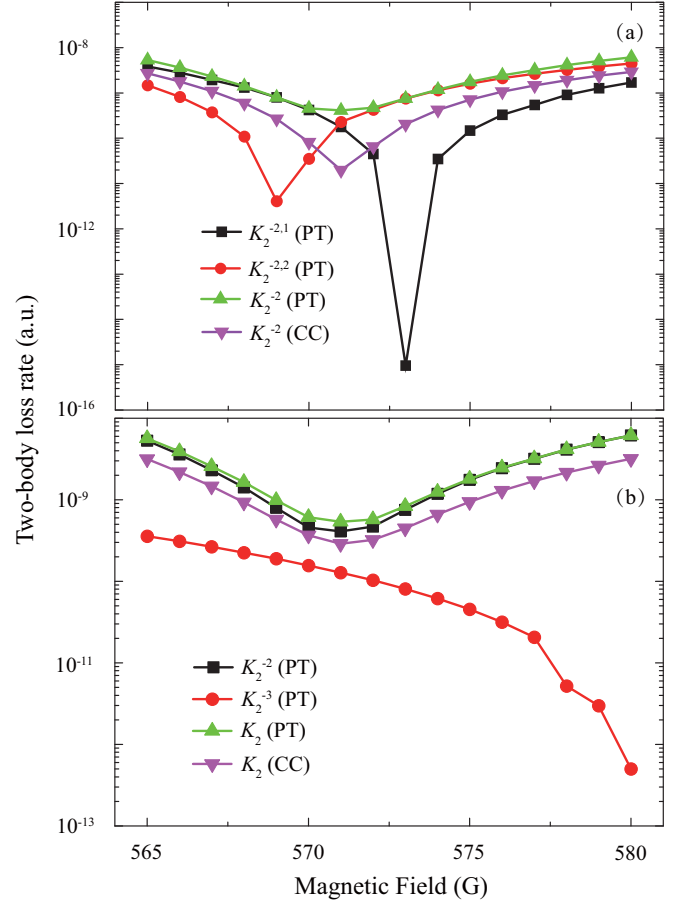

FIG. 7. The calculated two-body loss rates in the range from 565 to 580 G to outgoing channel $M_F = -2$ (a) and full loss channels (b).

except for the range near the Frs induced by the d-wave bound states of $M_F = -3$. It indicates the colliding atoms are more favourably decayed to open channel with lower energy beyond Frs.

The calculations with full loss channels show PT method is still considerable in multiloss channels by excluding interference of different open channels. We may ask a question: the full-channel wave functions in outgoing M_F can be replaced by the one in the exit channel? With this doubt we recalculate K_2(PT) with a single-channel wave function in corresponding outgoing M_F at the fields discussed above. We found the results only agree with CC at low magnetic fields and they differ greatly in other regions. This is because the Zeeman and hyperfine coupling is strong compared to SDIs at high fields and we cannot take it for granted that the loss to a particular M_F is just the sum of the loss to every channel. Besides, in the above discussion, we proposed the possibility to produce a minimum in two-body loss through introducing another similar adjustable loss process for only one outgoing channel case. However, the feasibility becomes complicated for more than one outgoing channel as the inelastic collisions of which could be influenced at different degrees by the introduced new loss process. One optional way is that we can create a minimum in the dominated loss channel in the case the loss to minor channels will not be enhanced obviously.

Experimentally suppressing SDIs-induced loss in ultracold diatomic collisions could be using a combination of electric and radio-frequency (RF) fields. The RF field can couple different M_F with the same partial wave by the R-independent interaction of RF photon with magnetic moment [3]. The electric field offers the coupling of different partial-waves in the same M_F via the R-dependent interaction of field with permanent dipole moment of diatom or static electric polarizabilities of atoms [53]. Therefore the incoming and outgoing channels are associated together in another way. This combination could create an indirect coupling which will not influence the elastic collision rate a lot but probably modify the inelastic scattering property obviously due to interference by tuning the electric and RF fields intensities.

IV. CONCLUSION

In summary, we investigated the SDIs induced two-body loss rates of ^{85}Rb in $|2, -2>$ ultracold collision by using improved PT and CC approaches. The two-body loss rates to the outgoing channel in $M_F = -3$ at three typical regions are investigated: lower magnetic field, near Fr and high magnetic field. It shows that by taking into account the full scattering wave function we can estimate SIDs-induced two-body loss rate for ultracold diatomic collisions in the presence of magnetic field with PT approach. The short range second-order SOC is demonstrated playing an important role in two-body loss process in ultracold ^{85}Rb diatomic collisions due to the interference between the loss induced by SOC and MDDI. Besides, we verified the pronounced dip in two-body loss rate around 571 G mainly comes from the superposition of losses from the two lower outgoing channels in $M_F = -2$ with close minima. Our calculations indicate beyond the Frs region the diatom collisions in energetically high Zeeman level prefer decaying to lower channel in the case several outgoing channel exist as well. Finally, we suggest the two-body loss could be suppressed by introducing another weak loss process due to the interference between two loss mechanisms. We also present a possible scheme to tune dipolar two-body loss in ultracold diatomic experiment.

[1] C. Chin, R. Grimm, P. Julienne, and E. Tiesinga, Rev. Mod. Phys. **82**, 1225 (2010).

[2] T. Xie, G.-R. Wang, W. Zhang, Y. Huang, and S.-L. Cong, Phys. Rev. A **84**, 032712 (2011).

[3] T. Xie, G.-R. Wang, Y. Huang, W. Zhang, and S.-L. Cong, J. Phys. B **45**, 145302 (2012).

[4] S. Dong, Y. Cui, C. Shen, Y. Wu, M. K. Tey, L. You, and B. Gao, Phys. Rev. A **94**, 062702 (2016).

[5] Y. Cui, C. Shen, M. Deng, S. Dong, C. Chen, R. Lü, B. Gao, M. K. Tey, and L. You, Phys. Rev. Lett. **119**, 203402 (2017).

[6] V. Barbé, A. Ciamei, B. Pasquiou, L. Reichsöllner, F. Schreck, P. S. Żouchowski, and J. M. Hutson, Nat. Phys. **14**, 881 (2018).

[7] A. Green, H. Li, J. H. S. Toh, X. Tang, K. McCormick, M. Li, E. Tiesinga, S. Kotochigova, and S. Gupta, arXiv:1912.04874v3.

[8] C. Chin, V. Vuletić, A. J. Kerman, S. Chu, E. Tiesinga, P. J. Leo, and C. J. Williams, Phys. Rev. A **70**, 032701 (2004).

[9] T. Hartmann, T. A. Schulze, K. K. Voges, P. Gersema, M. W. Gempel, E. Tiemann, A. Zenesini, and S. Ospelkaus, Phys. Rev. A **99**, 032711 (2019).

[10] H. Yang, D.-C. Zhang, L. Liu, Y.-X. Liu, J. Nan, B. Zhao, and J.-W. Pan, Science **363**, 261 (2019).

[11] A. Marte, T. Volz, J. Schuster, S. Dürr, G. Rempe, E. G. M. van Kempen, and B. J. Verhaar, Phys. Rev. Lett. **89**, 283202 (2002).

[12] V. Vuletić, A. J. Kerman, C. Chin, and S. Chu, Phys. Rev. Lett. **82**, 1406 (1999).

[13] H.-W. Cho, D. J. McCarron, M. P. Köppinger, D. L. Jenkin, K. L. Butler, P. S. Julienne, C. L. Blackley, C. R. LeSueur, J. M. Hutson, and S. L. Cornish, Phys. Rev. A **87**, 010703(R) (2013).

[14] M. Gröbner, P. Weinmann, E. Kirilov, H.-C. Nägerl, P. S. Julienne, C. R. LeSueur, and J. M. Hutson, Phys. Rev. A **95**, 022715 (2017).

[15] F. H. Mies, C. J. Williams, P. S. Julienne, and M. Krauss, J. Res. Natl. Inst. Stand. Technol. **101**, 521 (1996).

[16] P. J. Leo, E. Tiesinga, P. S. Julienne, D. K. Walter, S. Kadlecek, and T. G. Walker, Phys. Rev. Lett. **81**, 1389 (1998).

[17] S. Yi and L. You, Phys. Rev. A **63**, 053607 (2001).

[18] X.-C. Yao, R. Qi, X.-P. Liu, X.-Q. Wang, Y.-X. Wang, Y.-P. Wu, H.-Z. Chen, P. Zhang, H. Zhai, Y.-A. Chen, and J.-W. Pan, Nat. Phys. **15**, 570 (2019)

[19] L. Santos, G. V. Shlyapnikov, P. Zoller, and M. Lewenstein, Phys. Rev. Lett. **85**, 1791 (2000).

[20] M. A. Baranov, M. S. Mar'enko, V. S. Rychkov, and G. V. Shlyapnikov, Phys. Rev. A **66**, 013606 (2002).

[21] S. Hensler, J. Werner, A. Griesmaier, P. O. Schmidt, A. Gorlitz, and T. Pfau, Appl. Phys. B **77**, 765 (2002).

[22] N. Q. Burdick, Y. Tang, and B. L. Lev, Phys. Rev. X **6**, 031022 (2016).

[23] J. S. Krauser, J. Heinze, S. Götze, M. Langbecker, N. Fläschner, L. Cook, T. M. Hanna, E. Tiesinga, K. Sengstock, and C. Becker, Phys. Rev. A **95**, 042701 (2017).

[24] P. O. Fedichev, M. W. Reynolds, U. M. Rahmanov, and G. V. Shlyapnikov, Phys. Rev. A **53**, 1447 (1996).

[25] B. Pasquiou, G. Bismut, Q. Beaufils, A. Crubellier, E. Maréchal, P. Pedri, L. Vernac, O. Gorceix, and B. Laburthe-Tolra, Phys. Rev. A **81**, 042716 (2010).

[26] P. Xu, J. Yang, M. Liu, X. He, Y. Zeng, K. Wang, J. Wang, D. J. Papoular, G. V. Shlyapnikov, and M. Zhan, Nat. Commun. **6**, 7803 (2015).

[27] J. P. Burke, J. L. Bohn, B. D. Esry, and C. H. Greene, Phys. Rev. Lett. **80**, 2097 (1998).

[28] J. M. Vogels, C. C. Tsai, R. S. Freeland, S. J. J. M. F. Kokkelmans, B. J. Verhaar, and D. J. Heinzen, Phys. Rev. A **56**, R1067(R) (1997).

[29] S. L. Cornish, N. R. Claussen, J. L. Roberts, E. A. Cornell, and C. E. Wieman, Phys. Rev. Lett. **85**, 1795 (2000).

[30] S. T. Thompson, E. Hodby, and C. E. Wieman, Phys. Rev. Lett. **94**, 020401 (2005).

[31] T. Köhler, E. Tiesinga, and P. S. Julienne, Phys. Rev. Lett. **94**, 020402 (2005).

[32] C. L. Blackley, C. R. Le Sueur, J. M. Hutson, D. J. McCarron, M. P. Köppinger, H.-W. Cho, D. L. Jenkin, and S. L. Cornish, Phys. Rev. A **87**, 033611 (2013).

[33] R. J. Wild, P. Makotyn, J. M. Pino, E. A. Cornell, and D. S. Jin, Phys. Rev. Lett. **108**, 145305 (2012).

[34] D. A. Brue and J. M. Hutson, Phys. Rev. A **87**, 052709 (2013).

[35] Q. Beaufils, A. Crubellier, T. Zanon, B. Laburthe-Tolra, E. Maréchal, L. Vernac, and O. Gorceix, Phys. Rev. A **79**, 032706 (2009).

[36] C. Ticknor, C. A. Regal, D. S. Jin, and J. L. Bohn, Phys. Rev. A **69**, 042712 (2004).

[37] C. Strauss, T. Takekoshi, F. Lang, K. Winkler, R. Grimm, J. Hecker Denschlag, and E. Tiemann, Phys. Rev. A **82**, 052514 (2010).

[38] J. M. Hutson and S. Green, computer code MOLSCAT, version 14 (CCP6, Daresbury, 1994).

[39] B. R. Johnson, J. Comput. Phys. **13**, 445 (1973).

[40] J. M. Blatt, J. Comput. Phys. **1**, 382 (1967).

[41] K. Willner, O. Dulieu, and F. Masnou-Seeuws, J. Chem. Phys. **120**, 548 (2004).

[42] P. Pellegrini, M. Gacesa, and R. Côté, Phys. Rev. Lett. **101**, 053201 (2008).

[43] O. Dulieu and C. Gabbanini, Rep. Prog. Phys. **72**, 086401 (2009).

[44] N. Bouloufa, M. Pichler, M. Aymar, and O. Dulieu, Phys. Rev. A **83**, 022503 (2011).

[45] A. Ridinger, S. Chaudhuri, T. Salez, D. R. Fernandes, N. Bouloufa, O. Dulieu, C. Salomon, and F. Chevy, Europhys. Lett. **96**, 33001 (2011).

[46] N. Bouloufa-Maafa, M. Aymar, O. Dulieu, and C. Gabbanini, Laser Phys. **22**, 1502 (2012).

[47] M. Gacesa, S. Ghosal, J. N. Byrd, and R. Côté, Phys. Rev. A **88**, 063418 (2013).

[48] D. Borsalino, R. Vexiau, M. Aymar, E. Luc-Koenig, O. Dulieu, and N. Bouloufa-Maafa, J. Phys. B **49**, 055301 (2016).

[49] J. Vala, O. Dulieu, F. Masnou-Seeuws, P. Pillet, and R. Kosloff, Phys. Rev. A **63**, 013412 (2000).

[50] C. P. Koch, R. Kosloff, and F. Masnou-Seeuws, Phys. Rev. A **73**, 043409 (2006).

[51] T. Karman and J. M. Hutson, Phys. Rev. Lett. **121**, 163401 (2018).

[52] L. Lassablière and G. Quéméner, Phys. Rev. Lett. **121**, 163402 (2018).

[53] M. Marinescu and L. You, Phys. Rev. Lett. **81**, 4596 (1998).